

Hydrodynamic Analysis of Aircraft Water Supply

M. TÖPPEL, PROF. DR. E. PASCHE, DR. F. PUNTIGLIANO, M. RADA, DR. U. TESCHKE
Department of River and Coastal Engineering
Hamburg University of Technology
Denickestraße 22, 21073 Hamburg
GERMANY
<http://www.tu-harburg.de/wb>

Abstract: This paper describes a finite element model for the solution of one-dimensional unsteady flow in pipe-networks as well as a simulation scheme for air pressurized fluid tanks. These models can be used to simulate water consumption in airplanes, but are also applicable to other fields of interest, e.g. the calculation of pressure surges in tall buildings, in industrial plants or in urban water supply networks. With the presented finite element procedure, the system of nonlinear differential equations can be solved. Using an adaptive time-step control unsteady pipe flow can be simulated with a high resolution and a very high accuracy in short calculation time. Numerical results are compared to results of laboratory measurements.

Key-Words: water hammer, FEM, numerical simulation, one-dimensional pipe flow, transient flow, pressurized tank

1 Introduction

By amending the drinking water regulations all water supply systems in public transport systems like airplanes have to provide drinking water in the future. For this reason airlines have great interest in disinfection modules that can be installed in aircrafts. In addition to the development of an effective water disinfection, general investigations for the constructional improvement of existing water systems are necessary. For this reason the development of an efficient innovative application of pressure supply is demanded. Today's water systems in airplanes are supplied with pressure through a combination of engine bleed air and additional compressed air. During flight pressure is supplied mainly by bleed air while the compressors are used on the ground and on demand for supporting the pressure supply of bleed air. This technology has some disadvantages. To conduct bleed air from the engines to the water tank requires a complex system of pipelines and control valves. The valves have to reduce the pressure and if necessary they have to activate the compressors. Besides, the system must work in a broad spectrum of temperature. Experience shows that the necessary devices cause problems affecting the reliability of the pressure system.

A dynamically adaptable compressor system can replace the complex bleed air based pressure systems in future. A simplified structure is more favorable and more reliable, however at present it is not yet state of the art in aircraft construction.

In addition to the development of an innovative pressure system experimental investigations for the performance of different compressors as well as investigation of interaction effects between the subsystems pressure supply, water storage and water supply are necessary.

For the simulation of the dynamic interaction processes a numerical model was developed. In this model the one-dimensional NAVIER-STOKES-Equation applied to pipes is coupled with the gas dynamics of the pressure system. Thus, switching cycles of the compressors as well as the variation of the pressure in the system can be simulated very fast. With the numeric tool the water supply system as well as the control of the pressure supply can be optimized.

2 Numerical model for the pipe net

2.1 Governing differential equations

The basis for the computation of one-dimensional flow in pressure pipelines is a differential equation system, which consists of the momentum and the continuity equation:

$$\begin{aligned} \frac{\partial Q}{\partial t} + \frac{Q}{A} \frac{\partial Q}{\partial x} - \frac{Q}{A} \frac{\partial A}{\partial p} \frac{\partial p}{\partial t} - \frac{Q^2}{A^2} \frac{\partial A}{\partial x} + \frac{A}{\rho} \frac{\partial p}{\partial x} + gA \frac{\partial z}{\partial x} + gAS_F = 0 \\ \frac{\partial Q}{\partial x} - \frac{Q}{A} \frac{\partial A}{\partial x} + \frac{A}{\rho a^2} \left(\frac{\partial p}{\partial t} + \frac{Q}{A} \frac{\partial p}{\partial x} \right) = 0 \end{aligned} \quad (1)$$

where Q = discharge; g = acceleration of gravity; p = pressure; z = coordinate of height; S_F = friction slope; ρ = density; a = velocity of the pressure wave; x = coordinate axis along the pipe; t = time.

The friction slope S_F can be determined according to DARCY-WEISBACH with the following expression:

$$S_F = \frac{\lambda}{d} \frac{Q|Q|}{A^2 g} \quad (2)$$

2.2 Consideration of friction loss

For the calculation of the friction coefficient λ an equation is used that was developed by ZANKE:

$$\lambda_{\text{steady}} = (1 - \alpha) \left[\frac{64}{\text{Re}} \right] + \alpha \left[-2 \log \left(2,7 \frac{(\log(\text{Re}))^{1,2}}{\text{Re}} + \frac{k_s/d}{3,71} \right) \right]^{-2} \quad (3)$$

where α = weighing function; Re = Reynolds number; k_s = equivalent sand roughness; d = pipe diameter.

The explicit calculation of the friction coefficient as well as to have a continuously differentiable function for both laminar and turbulent flow conditions are advantages of equation (3).

Computations with this quasi-steady friction term however show only satisfying results for slow changes of the system-variables, for which the wall shear stress exhibits a quasi-steady behavior. Experiments showed that rapid changes result in larger discrepancies between measured and simulated parameters due to the steady or quasi-steady friction-coefficient.

Since many years researchers developed approaches for an unsteady friction factor. ZIELKE analytically found a term for laminar flow conditions. The friction term is related to the instantaneous mean flow velocity and to weighted past velocity changes.

BRUNONE developed a model, which relates the unsteady part of the friction coefficient to the instantaneous local acceleration $\partial v / \partial t$ and to the instantaneous convective acceleration $\partial v / \partial x$. The original model however exhibited weak points, since it failed to predict the correct sign of the convective term for particular flow and wave directions in acceleration and deceleration phases. The corrected formula is:

$$\lambda_{\text{unsteady}} = \lambda_{\text{steady}} + \frac{2kd}{v|v|} \left(\frac{\partial v}{\partial t} + a \cdot \text{sgn}(v) \cdot \left| \frac{\partial v}{\partial x} \right| \right) \quad (4)$$

where k = BRUNONE friction coefficient.

Equation (4) is transformed to a flow equation by substituting $Q = vA$, thus it can be written in the following way:

$$\lambda_{\text{unsteady}} = \lambda_{\text{steady}} + \frac{2kd}{Q|Q|} \left(A \frac{\partial Q}{\partial t} - Q \frac{\partial A}{\partial t} + a \cdot \text{sgn}(Q) \cdot \left| A \frac{\partial Q}{\partial x} - Q \frac{\partial A}{\partial x} \right| \right) \quad (5)$$

2.3 Solving the differential equations with the method of finite elements

For the simulation of unsteady pipe flow the method of finite elements is used. The pressure $p_{K,i}$ and the discharge $Q_{K,i}$ at every node are the variables to be determined. The system of differential equations can be applied on single pipelines for one-dimensional flow. At junctions a discontinuity of the discharge is encountered that cannot be calculated by one-dimensional finite elements. A solution is found by the use of algebraic equation for junctions as well as for all special elements of the pipe-network, e.g. for pumps, valves, tanks etc.

Another characteristic of the differential equation is the non-linearity of the momentum equation. For this reason the solution of the finite element formulation of the resulting set of equations is received with the iterative NEWTON-RAPHSON-procedure, which can be represented in the following form:

$$\begin{bmatrix} \frac{\partial f_{1,n}}{\partial x_{1,n}} & \dots & \frac{\partial f_{1,n}}{\partial x_{m,n}} \\ \vdots & & \vdots \\ \frac{\partial f_{m,n}}{\partial x_{1,n}} & \dots & \frac{\partial f_{m,n}}{\partial x_{m,n}} \end{bmatrix} \begin{bmatrix} x_{1,n+1} - x_{1,n} \\ x_{2,n+1} - x_{2,n} \\ \vdots \\ x_{m-1,n+1} - x_{m-1,n} \\ x_{m,n+1} - x_{m,n} \end{bmatrix} + \begin{bmatrix} f_{1,n} \\ f_{2,n} \\ \vdots \\ f_{m-1,n} \\ f_{m,n} \end{bmatrix} = \begin{bmatrix} 0 \\ 0 \\ \vdots \\ 0 \\ 0 \end{bmatrix} \quad (6)$$

where $f_{i,n}$ = finite element formulation of the differential and algebraic equations for each node; $x_{i,n+1}$ = solution of the variables for the next iteration step.

Advantages of the method of finite elements are the possibility to adjust the time-step and the element size. In combination with an adaptive time-step-control, a high accuracy of the solution is achieved and it is possible to simulate the interaction of the water system during a flight in very short calculation time.

2.4 Finite element formulation for the differential equations and their derivatives

This model uses a formulation based on the method of weighted residuals. In this method the differential equations are applied in integral notation. The shape functions N_n of the finite element approximation are used as the weighing parameters N^W . The contribution of a single element of length L can be defined as:

$$f_1 = \int_0^L N^W \left(\frac{\partial Q}{\partial t} + \frac{Q}{A} \frac{\partial Q}{\partial x} - \frac{Q}{A} \frac{\partial A}{\partial p} \frac{\partial p}{\partial t} - \frac{Q^2}{A^2} \frac{\partial A}{\partial x} + \frac{A}{\rho} \frac{\partial p}{\partial x} + gA \frac{\partial z}{\partial x} + gAS_F \right) dx \quad (7)$$

$$f_2 = \int_0^L N^W \left(\frac{\partial Q}{\partial x} - \frac{Q}{A} \frac{\partial A}{\partial x} + \frac{A}{\rho a^2} \left(\frac{\partial p}{\partial t} + \frac{Q}{A} \frac{\partial p}{\partial x} \right) \right) dx \quad (8)$$

In order to solve the equation system with the NEWTON-RAPHSON-procedure, equation (7) and (8) have to be differentiated to pressure and discharge at all nodes n.

With the relations:

$$\frac{\partial y(x)}{\partial y_n} = N_n \quad (9)$$

$$\frac{\partial f(y(x))}{\partial y_n} = \frac{\partial f(y(x))}{\partial y(x)} \frac{\partial y(x)}{\partial y_n} = N_n \frac{\partial f(y(x))}{\partial y} \quad (10)$$

$$\frac{\partial^2 y(x)}{\partial y_n \partial x} = \frac{\partial}{\partial x} \left(\frac{\partial y(x)}{\partial y_n} \right) = \frac{\partial N_n}{\partial x} \quad (11)$$

the derivatives are:

$$\frac{\partial f_1}{\partial p_n} = \int_0^L N^w N_n \left[\begin{array}{c} \frac{Q}{A^2} \frac{\partial A}{\partial p} \left(\frac{\partial A}{\partial p} \frac{\partial p}{\partial t} - \frac{\partial Q}{\partial x} - A \frac{\theta}{\Delta t} \right) \\ - \frac{Q}{A} \frac{\partial^2 A}{\partial p^2} \frac{\partial p}{\partial t} - \frac{Q^2}{A^2} \frac{\partial^2 A}{\partial p \partial x} \\ + \frac{\partial A}{\partial p} \left(\frac{1}{\rho} \frac{\partial p}{\partial x} + g \frac{\partial z}{\partial x} + g S_f \right) \\ - \frac{A}{\rho^2} \frac{\partial \rho}{\partial p} \frac{\partial p}{\partial x} + \frac{1}{N_n} \frac{A}{\rho} \frac{\partial N_n}{\partial x} + g A \frac{\partial S_f}{\partial p} \end{array} \right] dx \quad (12)$$

$$\frac{\partial f_1}{\partial Q_n} = \int_0^L N^w N_n \left[\begin{array}{c} \frac{\theta}{\Delta t} + \frac{1}{A} \frac{\partial Q}{\partial x} + \frac{Q}{A} \frac{1}{N_n} \frac{\partial N_n}{\partial x} \\ - \frac{1}{A} \frac{\partial A}{\partial p} \frac{\partial p}{\partial t} - 2 \frac{Q}{A^2} \frac{\partial A}{\partial x} + g A \frac{\partial S_f}{\partial Q} \end{array} \right] dx \quad (13)$$

$$\frac{\partial f_2}{\partial p_n} = \int_0^L N^w N_n \left[\begin{array}{c} \frac{A}{\rho a^2} \frac{\partial p}{\partial t} \left(\frac{1}{A} \frac{\partial A}{\partial p} - \frac{1}{\rho} \frac{\partial p}{\partial p} - \frac{2}{a} \frac{\partial a}{\partial p} \right) \\ - \frac{Q}{\rho a^2} \frac{\partial p}{\partial x} \left(\frac{1}{\rho} \frac{\partial p}{\partial p} + \frac{2}{a} \frac{\partial a}{\partial p} \right) \\ + \frac{A}{\rho a^2} \left(\frac{\theta}{\Delta t} + \frac{1}{N_n} \frac{Q}{A} \frac{\partial N_n}{\partial x} \right) \\ + \frac{Q}{A} \left(\frac{1}{A} \frac{\partial A}{\partial p} \frac{\partial A}{\partial x} - \frac{\partial^2 A}{\partial p \partial x} - \frac{1}{N_n} \frac{\partial N_n}{\partial x} \frac{\partial A}{\partial p} \right) \end{array} \right] dx \quad (14)$$

$$\frac{\partial f_2}{\partial Q_n} = \int_0^L N^w N_n \left[\frac{1}{N_n} \frac{\partial N_n}{\partial x} + \frac{1}{\rho a^2} \frac{\partial p}{\partial x} - \frac{1}{A} \frac{\partial A}{\partial x} \right] dx \quad (15)$$

For the time integration scheme a finite difference expression is used:

$$\frac{\partial z(t + \Delta t)}{\partial t} = \theta \left(\frac{z(t + \Delta t) - z(t)}{\Delta t} \right) + (1 - \theta) \frac{\partial z(t)}{\partial t} \quad (16)$$

where θ = relaxation coefficient ($1 \leq \theta \leq 2$).

From this expression the following equations result which are used to calculate the derivatives of the finite element formulation:

$$\begin{aligned} \frac{\partial}{\partial p_n(t + \Delta t)} \left(\frac{\partial p(t + \Delta t)}{\partial t} \right) &= N_n(x) \frac{\theta}{\Delta t} \\ \frac{\partial}{\partial Q_n(t + \Delta t)} \left(\frac{\partial Q(t + \Delta t)}{\partial t} \right) &= N_n(x) \frac{\theta}{\Delta t} \end{aligned} \quad (17)$$

The extreme complexity of equation 7, 8 and 12 to 15 makes an exact integration impossible. Therefore, the integrals are solved by numerical integration, e.g. by GAUSS-LEGENDRE integration.

3 Numerical model for pressurized water tanks

This mathematical model is able to simulate the pressurization process in tanks during flight and on ground. Fig. 1 shows the assumed system architecture.

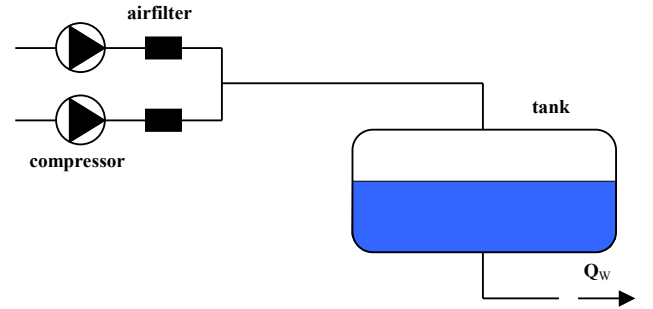


Fig. 1: Simplified form of the architecture of the pressurization subsystem

For the simulation the performance of the compressors and the pressure loss at the air-filters are boundary conditions. It is assumed that the pressurization process is isothermic.

The General Law of Gases is applicable and the time derivative of this law is:

$$\frac{\partial p}{\partial t} \rho - \frac{\partial \rho}{\partial t} p = 0 \quad (18)$$

where p = air pressure and ρ = air density.

The total volume of the tank is constant and given by $V_T = V_w + V$. The time derivative of this equation is:

$$\frac{\partial V_w}{\partial t} + \frac{\partial V}{\partial t} = Q_w + \frac{\partial V}{\partial t} = 0 \quad (19)$$

where V = air volume; V_w = volume of the fluid; V_T = volume of the tank.

The air mass is given by $m = \rho V$, so that the time derivative is expressed by:

$$\frac{\partial m}{\partial t} = \rho \frac{\partial V}{\partial t} + V \frac{\partial \rho}{\partial t} \quad (20)$$

The mass flow depends on the performance of the compressors and on their steering (switch on/off) points. These equations constitute a linear equation system with the following unknowns $\partial p/\partial t$, $\partial \rho/\partial t$ and $\partial V/\partial t$ that can be solved by numerical integration. The variables pressure p and flow Q_w depend on the consumption and therefore interact with the numerical model of the pipe-net.

4 Numerical and experimental results

4.1 Pressure surges

The differential equation system is used to calculate pressure surges in pipe-networks. Pressure surges arise for example after fast closing or opening of valves as well as switching on or off pumps. The reason is the mass inertia of the fluid.

For comparing the numerical results, an experimental apparatus for investigating water hammer was constructed (Fig. 2). A straight 15.05 m long steel pipe of 17.3 mm internal diameter and 1.9 mm wall thickness was connected to a 370 l pressurized water-tank.

The valve belongs to an aircraft toilet and has a closure time of 0.03 seconds.

The pressure and the discharge were recorded with a frequency of 333 Hz.

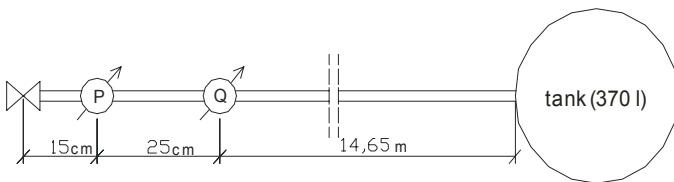


Fig. 2: Architecture of the experimental apparatus

Several water hammer experiments were run to compare numerical and measured results. Starting with a pressure

of 1 bar, the valve is opened after 0.5 seconds and closed again after another 0.5 seconds.

The calculated discharge (Fig. 3) is almost identical with the measured data. The small difference at the closure of the valve is due to an internal delay of the flow meter.

When the valve is opened the pressure changes until after some time steady flow conditions have developed. After rapid closure of the valve a transient event is initiated and the water hammer wave travels between the closed valve and the tank.

Computational results of the pressure decrease after the opening as well as the increase of the pressure after rapid closure of the valve agree to the measured values. Differences arise after the first pressure wave is reflected at the valve (Fig. 4). Since the pressure cannot be lower than the vapor pressure of the liquid, cavitation will occur. Therefore the reflection of the pressure wave is disturbed in a way that cannot be accurately simulated with a one-dimensional flow model. For most transient analysis the height of the initial pressure wave is most important. Therefore the computational model shows good results by comparing to measured data.

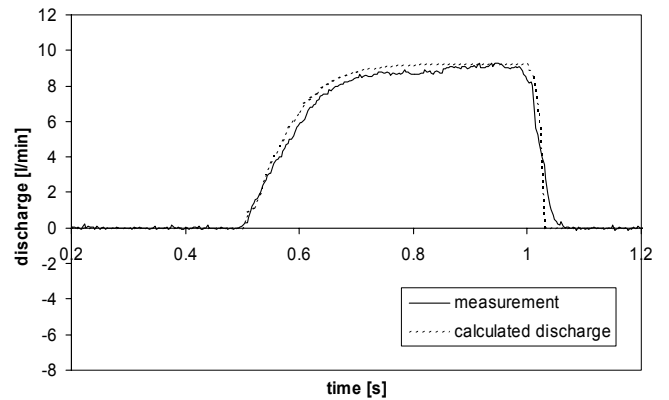


Fig. 3: Comparison of measured and calculated discharge

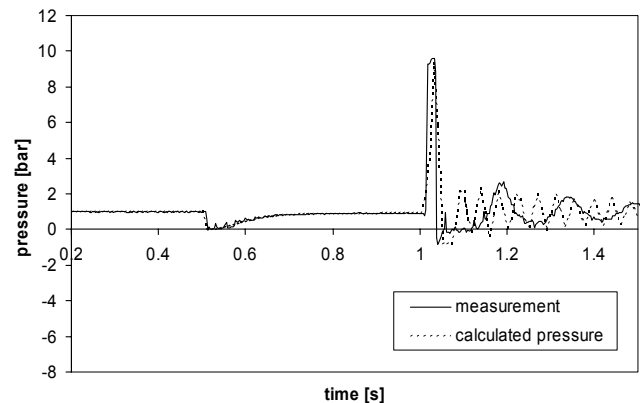


Fig. 4: Comparison of measured and calculated pressure

Without cavitation effects, the reflection of the pressure wave can also be accurately simulated (Fig. 5). For this test measured data from BERGANT ET AL. was compared to the simulation.

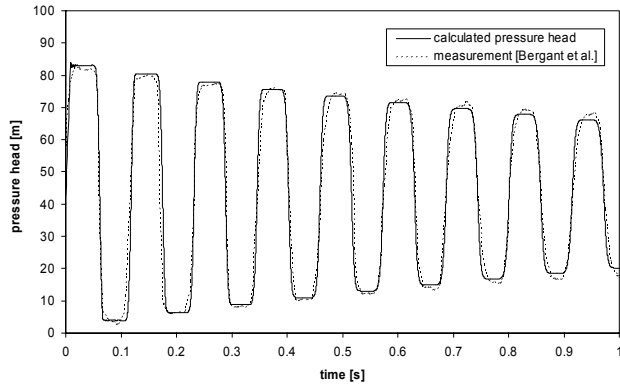


Fig. 5: Comparison of measured and calculated pressure heads (measurements from BERGANT et al.)

4.2 Pressurization of an aircraft water tank

In order to demonstrate the pressurization process in an aircraft tank, a simulation was done for a 12 hours flight. For this example a 500 l tank containing 400 l water was assumed.

The cabin pressure varies from 550 Pa (8.0 psia) at the starting point (e.g. at La Paz) over 760 Pa (11.0 psia) cabin pressure during the flight to 1000 Pa (14.5 psia) at the destination airport.

During the first minutes of the flight the tank is pressurized up to 40 psig which is the limit of the first compressor when it will switch off. If the pressure decreases beneath 34 psig it will switch on again. The working range of the second compressor is 32 to 38 psig. Four times water is withdrawn from the tank. The pressure decreases until one of the two compressors will switch on.

The tank pressure, the cabin pressure and the consumption are displayed in Fig. 6, the according water volume in the tank and the numbers of active compressors are presented in Fig. 7.

With the presented simulation tool it is possible to optimize the activation of the compressors in dependency of the air pressure, the switching range, the consumption and the volume of the water tank.

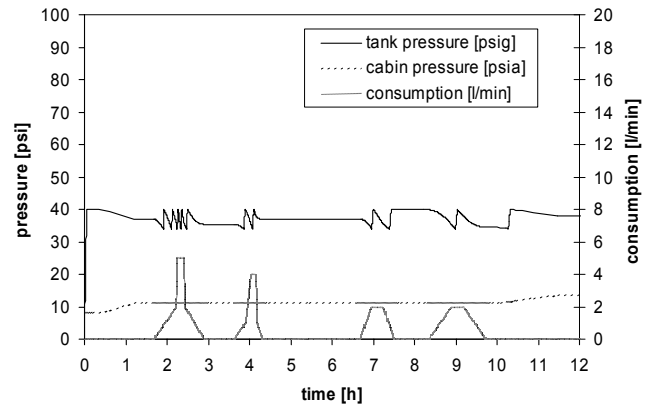


Fig. 6: Tank pressure, cabin pressure and consumption during a simulated flight

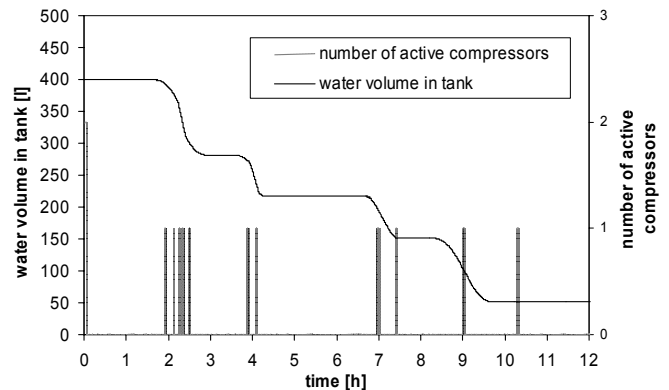


Fig. 7: Number of active compressors and water volume in tank during a simulated flight

5. Convergence and stability

The numerical solution with the finite element method should satisfy convergence and stability criteria. Convergence relates to the behavior of the solution when Δt and Δx tend to zero while stability is concerned with round-off error growth.

The convergence of the presented model was examined for a number of different Δt and Δx sizes. The influence of the element length Δx is less important than the influence of the time step Δt , especially for highly unsteady processes.

The method showed high accuracy and convergence as well as a numerically stable behavior.

6. Conclusion

With the presented numerical methods it is possible to simulate unsteady pipe flow with a high resolution and a very satisfying accuracy in short calculation time. The adaptive time-step-control allows to simulate flights of

several hours whereas transients are accurately reproduced using an unsteady friction factor.

Thus, the water consumption in airplanes can be simulated particularly close-to-reality, whereby a suitable and reliable solution for the pressure supply is expected for aviation water systems. The simulation of unsteady pipe flow in dependency of the pressurization of the tank allows to optimize the activation process of the compressors.

In addition, the numerical model can be applied to other applications, for example calculation of pressure surges in tall buildings or industrial plants with expanded and strongly meshed fluid supply networks as well as calculation of pressure and flow distribution in urban water supply networks.

References:

- [1] Bergant A., Simpson A.R., Vitkovsky J.: Developments in unsteady pipe flow friction modeling, *Journal of Hydraulic Research*, Vol. 39, No. 3, 2001, pp. 249-257
- [2] Brunone B., Golia U.M., Greco M.: Some remarks on the momentum equation for fast transients, *Int. Meeting on Hydraulic Transients with Column Separation*, 9th Round Table, IAHR, Valencia, Spain, 1991, pp. 201-209
- [3] Chaudhry M. H.: *Applied Hydraulic Transients*, Second Edition, Van Nostrand Reinhold Company Inc., New York, 1987
- [4] Larock B. E., Jeppson R. W., Watters G. Z.: *Hydraulics of Pipeline Systems*, CRC Press, Boca Raton, 2000
- [5] Martin H., Pohl R., u.a.: *Technische Hydromechanik Band 4, Hydraulische und numerische Modelle*, 1. Auflage, Verlag Bauwesen, Berlin, 2000
- [6] Pezzinga G.: Discussion: Developments in unsteady pipe flow friction modelling, *Journal of Hydraulic Research*, Vol. 40, No. 5, 2002, p. 650
- [7] Wylie E. B., Streeter V. L., Suo L.: *Fluid Transients in Systems*, Prentice Hall, Englewood Cliffs, New Jersey, 1993
- [8] Zanke U. C. E.: *Hydromechanik der Gerinne und Küstengewässer: Für Bauingenieure, Umwelt- und Geowissenschaftler*, Parey Buchverlag im Blackwell Wissenschafts-Verlag GmbH, Berlin, 2002
- [9] Zielke W.: *Elektronische Berechnung von Rohr- und Gerinneströmungen*, Erich Schmidt Verlag, Berlin, 1974